

The Spindle Checkpoint Functions of Mad3 and Mad2 Depend on a Mad3 KEN Box-mediated Interaction with Cdc20-Anaphase-promoting Complex (APC/C)^{*[5]♦}

Received for publication, May 9, 2008, and in revised form, June 12, 2008. Published, JBC Papers in Press, June 13, 2008, DOI 10.1074/jbc.M803594200

Matylda Sczaniecka^{‡1}, Anna Feoktistova[§], Karen M. May^{‡2}, Jun-Song Chen[§], Julie Blyth[‡], Kathleen L. Gould^{§3}, and Kevin G. Hardwick^{‡4}

From the [‡]Wellcome Trust Centre for Cell Biology, Institute of Cell Biology, University of Edinburgh, EH9 3JR, United Kingdom and the [§]Howard Hughes Medical Institute (HHMI) and Department of Cell and Developmental Biology, Vanderbilt University School of Medicine, Nashville, Tennessee 37232

Mitotic progression is driven by proteolytic destruction of securin and cyclins. These proteins are labeled for destruction by an ubiquitin-protein isopeptide ligase (E3) known as the anaphase-promoting complex or cyclosome (APC/C). The APC/C requires activators (Cdc20 or Cdh1) to efficiently recognize its substrates, which are specified by destruction (D box) and/or KEN box signals. The spindle assembly checkpoint responds to unattached kinetochores and to kinetochores lacking tension, both of which reflect incomplete biorientation of chromosomes, by delaying the onset of anaphase. It does this by inhibiting Cdc20-APC/C. Certain checkpoint proteins interact directly with Cdc20, but it remains unclear how the checkpoint acts to efficiently inhibit Cdc20-APC/C activity. In the fission yeast, *Schizosaccharomyces pombe*, we find that the Mad3 and Mad2 spindle checkpoint proteins interact stably with the APC/C in mitosis. Mad3 contains two KEN boxes, conserved from yeast Mad3 to human BubR1, and mutation of either of these abrogates the spindle checkpoint. Strikingly, mutation of the N-terminal KEN box abolishes incorporation of Mad3 into the mitotic checkpoint complex (Mad3-Mad2-Slp1 in *S. pombe*, where Slp1 is the Cdc20 homolog that we will refer to as Cdc20 hereafter) and stable association of both Mad3 and Mad2 with the APC/C. Our findings demonstrate that this Mad3 KEN box is a critical mediator of Cdc20-APC/C inhibition, without which neither Mad3 nor Mad2 can associate with the APC/C or inhibit anaphase onset.

typically leads to disease or cell death (1). To ensure that their genomes are replicated, repaired, and segregated with high fidelity, cells have evolved checkpoint controls. The spindle assembly checkpoint (SAC)⁵ delays anaphase onset until all sister chromatid pairs are bioriented on the mitotic spindle (2–4). The SAC works by preventing activation of the ubiquitin-protein isopeptide ligase (E3) known as the anaphase-promoting complex or cyclosome (APC/C (5)). In order for the APC/C to become active, it must interact with a transiently available activator; early in mitosis, this is Slp1/Cdc20, and later in mitosis and in G₁, it switches to Ste9/Cdh1 (6–8).

Cdc20 is the key target of the SAC (9, 10). The Mad2 and Mad3/BubR1 checkpoint proteins bind to and inhibit Cdc20, but their molecular mechanism(s) of inhibition remain incompletely understood. They could act by simply sequestering the APC/C activator or by otherwise preventing processive polyubiquitination of mitotic APC/C substrates. The APC/C substrates that must be polyubiquitinated and destroyed for mitosis to be completed are securin (Cut2/Pds1) and cyclin (Cdc13/Clb2) (11–13). APC/C substrates contain destruction signals, usually referred to as destruction (D) boxes, and KEN boxes (14, 15). These signals are recognized by APC/C activators (16–19), but it has also been shown that the vertebrate APC/C is capable of recognizing destruction motifs directly, in a Cdc20/Cdh1-independent manner (20).

Current models of SAC mechanism highlight the role of Mad2 in Cdc20 inhibition. A stable kinetochore-bound Mad1-Mad2 complex recruits additional Mad2 molecules, which then become primed for Cdc20 binding and inhibition (21–24). However, it is clear that the Mad3/BubR1 spindle checkpoint component also has a central role to play in Cdc20 inhibition (25–29). In fission yeast, Mad3 is the only checkpoint protein required for the overexpression of Mad2 to induce a metaphase arrest (28), indicating that a Mad2-Cdc20 complex is insufficient for checkpoint arrest *in vivo*. In addition, it has been shown that the mitotic checkpoint complex (MCC, typically

It is critical that cells segregate their chromosomes perfectly in every mitosis. Segregation errors result in aneuploidy, which

* This work was supported by grants from the HHMI (to J. S. C., A. F., and K. L. G.) and the Wellcome Trust (to J. B., K. M., and K. G. H.). The costs of publication of this article were defrayed in part by the payment of page charges. This article must therefore be hereby marked "advertisement" in accordance with 18 U.S.C. Section 1734 solely to indicate this fact.

♦ This article was selected as a Paper of the Week.

Author's Choice—Final version full access.

[5] The on-line version of this article (available at <http://www.jbc.org>) contains three supplemental figures.

¹ A graduate student funded by the Darwin Trust of Edinburgh. Present address: Royal (Dick) School of Veterinary Studies, The University of Edinburgh, Easter Bush Veterinary Centre, Roslin, EH25 9RG, UK.

² Funded by an Human Frontier Science Program grant.

³ An Investigator of the HHMI.

⁴ To whom correspondence should be addressed: Tel.: 44-131-650-7091; Fax: 44-131-650-7037; E-mail: Kevin.Hardwick@ed.ac.uk.

⁵ The abbreviations used are: SAC, spindle assembly checkpoint; APC/C, anaphase-promoting complex/cyclosome; MCC, mitotic checkpoint complex; Mad, mitotic arrest-defective; TAP, tandem affinity purification; GFP, green fluorescent protein; HTB, His₆-TEV-biotin; TEV, tobacco etch virus; PIPES, 1,4-piperazinediethanesulfonic acid; HA, hemagglutinin; DAPI, 4',6-diamidino-2-phenylindole.

TABLE 1
Yeast strains

KP135	<i>mad3Δ::ura4 ade6-210 leu1-32 ura4-D18</i>
KP361	<i>nda3-KM311 mad3-GFP::his3 leu1-32 ura4-D18</i>
YJB43	<i>mad3-GFP::his3 leu1-32 ura4-D18</i>
YJB122	<i>mad3-KEN20-GFP::his3 leu1-32 ura4-D18</i>
YJB84	<i>mad3-KEN271-GFP::his3 leu1-32 ura4-D18</i>
MS199	<i>slp1-HA::kan^r ade6-210 leu1-32 ura4-D18 his3-D1 arg3-D4 pN70-K0</i>
MS234	<i>mad3-GFP::his3 leu1-32 ura4-D18 pN70-K0</i>
MS209	<i>slp1-HA::kan^r mad3-GFP::his3 ade6-210 leu1-32 ura4-D18 his3-D1 pN70-K0</i>
MS207	<i>slp1-HA::kan^r mad3-KEN20-GFP::his3 ade6-210 leu1-32 ura4-D18 his3-D1 pN70-K0</i>
MS208	<i>slp1-HA::kan^r mad3-KEN271-GFP::his3 ade6-210 leu1-32 ura4-D18 his3-D1 pN70-K0</i>
MS196	<i>lid1-TAP::kan^r mad3-GFP::his3 leu1-32 ade6-210 pN70-K0</i>
MS202	<i>lid1-TAP::kan^r mad3-KEN20-GFP::his3 leu1-32 ade6-210 pN70-K0</i>
MS203	<i>lid1-TAP::kan^r mad3-KEN271-GFP::his3 leu1-32 ade6-210 pN70-K0</i>
MS201	<i>lid1-TAP::kan^r mad3-KEN20/271-GFP::his3 leu1-32 ade6-210 pN70-K0</i>
MS221	<i>lid1-TAP::kan^r mad3-GFP::his3 mad2::ura4 leu1-32 ade6-210 pN70-K0</i>
MS222	<i>lid1-TAP::kan^r mad3-GFP::his3 bub3::ura4 leu1-32 ade6-210 pN70-K0</i>
MS254	<i>lid1-TAP::kan^r mad3-GFP::his3 slp1-362 leu1-32 ade6-210</i>
MS186	<i>lid1-TAP::kan^r mad3-GFP::his3 mts3-1 leu1-32 ade6-210</i>
MS182	<i>lid1-TAP::kan^r mad3-KEN20-GFP::his3 mts3-1 leu1-32 ade6-210</i>
MS187	<i>lid1-TAP::kan^r mad3-KEN271-GFP::his3 mts3-1 leu1-32 ade6-210</i>
MS194	<i>lid1-TAP::kan^r mad3-KEN20/271-GFP::his3 mts3-1 leu1-32 ade6-210</i>
MS215	<i>slp1-HA::kan^r mad3-GFP::his3 bub3::ura4 leu1-32 ade6-210 pN70-K0</i>
MS284	<i>slp1-HA::kan^r mad3-GFP::his3 mad1::ura4 leu1-32 ade6-210 pN70-K0</i>
MS291	<i>slp1-HA::kan^r mad3-GFP::his3 mph1::mat^r, leu1-32, ade6-210 pN70-K0</i>
MS292	<i>slp1-HA::kan^r mad3-GFP::his3 bub1::ura4 leu1-32 ade6-210 pN70-K0</i>
KMY438	<i>nda3-KM311 mad3::ura4 leu1-32 ura4-D18</i>
KMY419	<i>nda3-KM311 mad3-KEN20AAA-GFP::his3 leu1-32 ura4-D18</i>
KMY446	<i>nda3-KM311 mad3-KEN271AAA-GFP::his3 leu1-32 ura4-D18</i>
KGY2152	<i>lid1-TAP::kan^r nda3-KM311 leu1-32 h⁻</i>
KGY6130	<i>nda3-KM311 lid1-Myc₁₃ mad2-GFP h⁺</i>
KGY6186	<i>cdc25-22 lid1-Myc₁₃ slp1-HA₃ h⁻</i>
KGY6343	<i>mad3-TAP::kan^r nda3-KM311 h⁻</i>
KGY7024	<i>mad2-HTB::kan^r lid1-Myc₁₃ nda3-KM311 ade6-M210 leu1-32 ura4-D18 h⁻</i>
KGY7104	<i>mad2-HTB::kan^r lid1-Myc₁₃ mts3-1 ade6-M210 leu1-32 ura4-D18 h⁻</i>

Mad3/BubR1-Bub3-Mad2-Cdc20) is a far more potent inhibitor than Mad2 *in vitro* (26, 30).

Here we show that both Mad3 and Mad2 can stably interact with the APC/C during fission yeast mitosis. The Mad3-APC/C interaction is dependent on Cdc20 and Mad2. Mutation of an N-terminal Mad3 KEN box prevents stable Mad3-Cdc20 binding, as well as Mad3 and Mad2 binding to APC/C, and abrogates the spindle checkpoint. We demonstrate that the N-terminal Mad3 KEN box, which is conserved from yeast Mad3 to human BubR1, is a critical link required for the concerted actions of Mad3 and Mad2 in checkpoint inhibition of Cdc20-APC/C.

EXPERIMENTAL PROCEDURES

Mitotic Arrests—Yeast strains are listed in Table 1. *nda3-KM311(cs)* cells were grown in rich medium (yeast extract plus supplements (YES)) at 30 °C to a density of 2×10^6 and then shifted to 18 °C for 8 h. For the viability assay, 200 cells were plated on YES and grown at 32 °C. For microscopy, cells were rapidly fixed in ice-cold 100% methanol and mounted with 1 mg/ml DAPI (Sigma). For pREP1-N70-K0, pREP3x-Mad2, and pREP41x-Mph1 overexpression arrests, precultures were grown in *Schizosaccharomyces pombe* minimal glutamate medium supplemented with 5 μ M thiamine for 24 h. Cells were then washed twice with the same medium lacking thiamine, and fresh media were inoculated at 2×10^5 /ml and incubated for 16–18 h (for Mad2 and Mph1) or 14–16 h (for N70-K0) at 30 °C.

The *cdc13* (cyclin B) construct used has all of the N70 lysines replaced with arginine (K0-N70), so as not to deplete cellular ubiquitin pools, and cells accumulate in metaphase when it is overpro-

duced (35). This is because the D box of the overexpressed cyclin titrates out Cdc20-APC/C, and as a result, other substrates such as Cut2 (securin) are not ubiquitinated efficiently.

Temperature-sensitive mutants were first cultured in YES overnight at 25 °C. *slp1-362* cultures (with an A_{600} of 0.2–0.4) were shifted to their restrictive temperature of 36 °C for 3 h. Typically 200-ml cultures were used for these experiments.

Immunoprecipitations—0.1 g of pellets of cells were resuspended in 300 μ l of ice-cold lysis buffer (50 mM Hepes, pH 7.6, 75 mM KCl, 1 mM MgCl₂, 1 mM EGTA, 0.1% Triton X-100, 1 mM Pefabloc (Roche Applied Science) and LPC (10 mg/ml each of leupeptin, pepstatin, and chymostatin, Roche Applied Science)) and bead-beaten with 0.5 mm of zirconia/silica beads (BioSpec Products) twice for 30 s. Extracts were clarified, and dithiothreitol was added to a final concentration of 0.5 mM. Protein A Dynabeads (Dyna) were preincubated with anti-GFP (Invitrogen) or anti-HA (Roche Applied Science) antibodies and washed twice (first wash, phosphate-buffered saline, 0.1% Triton X-100; second wash, lysis buffer). For tandem affinity purification (TAP)-tagged strains, Dynabeads (Dyna) coupled to IgG were used. Immunoprecipitations were performed for 2 h at 4 °C and washed, and proteins were eluted from the beads by incubating for 15 min at room temperature with SDS sample buffer containing 5% β -mercaptoethanol. Samples were analyzed by SDS-PAGE on 15% gels. Quantitative immunodepletion was carried out on Mad2 tagged at its endogenous locus with His₆-TEV-biotin (HTB) (60) using streptavidin-coated magnetic beads. The amount of Mad2-HTB and Lid1-Myc₁₃ in each lysate and brought down by beads was determined by immunoblotting and quantification on an Odyssey machine.

A

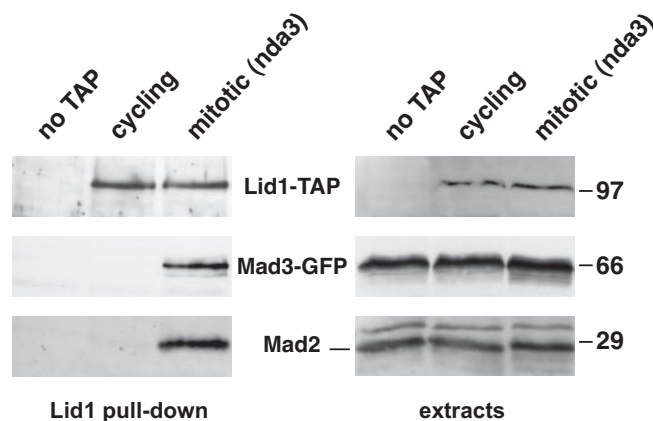
Component	<i>lid1-TAP nda3-KM311</i>		<i>mad3-TAP nda3-KM311</i>	
	I ^a	II ^b	I ^a	II ^b
Cut4	37.7	52	38.8	53
Apc2	42.7	27	38.6	24
Nuc2	53.4	39	48.1	37
Lid1	28.5	24	29.9	24
Apc5	52.4	36	41.7	30
Cut9	44	30	47.2	33
Cut23	47.4	29	44.4	23
Apc10	41.8	4	38.1	4
Apc11	30.9	3	17.0	2
Hcn1	53.8	8	81.3	9
Apc13	22.2	4	53.3	5
Apc14	45.8	5	57.0	7
Apc15	22.1	4	12.5	3
Slp1	41	14	45.3	17
Mad2	25.6	6	39.4	8
Mad3	49	16	56.5	20

^aPercentage of sequence coverage of each identified protein by mass spectrometry.

^bNumber of unique tryptic peptides of each identified protein by mass spectrometry.

FIGURE 1. *S. pombe* Mad3 and Mad2 stably interact with mitotic APC/C. A, Lid1-TAP and Mad3-TAP purifications were performed from mitotically arrested *S. pombe* strains. The TAP eluates were subjected to trypsin digestion and MudPIT mass spectrometric analysis. The sequence coverage and unique peptide numbers are shown. The data for *lid1-TAP nda3-KM311*, and *mad3-TAP nda3-KM311* were compiled from three experiments and one separate experiment, respectively. Lid1 is Apc4, and Slp1 is fission yeast Cdc20. B, Lid1-TAP was pulled down from cycling and mitotic (*nda3* arrested) cells, separated by SDS-PAGE, and immunoblotted for Lid1-TAP and associated Mad3-GFP and Mad2. The *right hand blots* are of the whole cell extracts.

B



Analysis of TAP Complexes by Mass Spectrometry—TAP complexes were isolated and analyzed using mass spectrometry as described previously (33). All tandem spectra were searched against the *S. pombe* protein data base using the SEQUEST algorithm and were then processed using CHIPS program (jointly developed by Vanderbilt University Mass Spectrometry Research Center and the University of Arizona). The following filter settings were used: Xcorr ≥ 1 for singly charged peptides; Xcorr ≥ 1.8 for doubly charged peptides; Xcorr ≥ 2.5 for triply charged peptides; and Sp ≥ 350 and Rsp ≤ 5 for peptides of all charge states.

Sucrose Gradients—Cell extracts were made by grinding cells in liquid nitrogen with a pestle and mortar. Lysis buffer was 50 mM Hepes (7.6), 75 mM KCl, 1 mM MgCl₂, 1 mM EGTA, 0.1% Triton X-100, 1 mM Pefabloc (Roche Applied Science), LPC (10 μ g/ml each of leupeptin, pepstatin, and chymostatin, Roche Applied Science), 0.5 mM dithiothreitol. Extracts were clarified by spinning at 13,000 rpm for 15 min. 100 μ l of extract were then fractionated on 10–40% sucrose gradients by spinning at 55,000 rpm for 5 h at 4 °C in a Beckman TLS55 rotor. 100- μ l fractions were collected and analyzed by immunoblotting.

Immunostaining—10–20 ml of an overnight culture were fixed with –80 °C cold methanol and washed twice in PEM (100 mM PIPES, pH 7 (sodium salt), 1 mM MgSO₄, 1 mM EGTA), and cell walls were digested with 0.4 mg/ml Zymolyase (MP Bio-medicals). Cells were then washed, blocked with Blotto (4% dried milk in phosphate-buffered saline + 0.1% Tween) for 1 h, and incubated with TAT1 (mouse anti-tubulin) antibody (1:50) for 16 h (kindly provided by Keith Gull, Oxford, UK). Anti-mouse secondary antibody (Alexa Fluor – Molecular Probes) was used at 1:100 for 1 h. Mitotic spindles were visualized using an Intelligent Imaging Innovations Marianas microscope (Zeiss Axiovert 200M, using a $\times 100$ 1.3NA objective lens), CoolSnap CCD, and Slidebook software (Intelligent Imaging Innovations, Inc., Boulder, CO). 300 cells were counted for each sample.

Cycloheximide Chase Experiments—To measure the rates of protein turnover during mitosis, 100 ml of *S. pombe* cultures were arrested using the pN70-K0 plasmid (35). A 10-ml sample was collected and centrifuged, and the pellet was frozen on dry ice. Next, cycloheximide was added to the remaining culture to a final concentration of 100 mg/ml to block new protein synthesis. 10-ml samples were collected at 5-, 10-, or 15-min intervals and centrifuged, and pellets were stored at –80 °C for further analysis. Protein extracts were prepared by ribolysing cells with zirconia-silica beads in SDS sample buffer.

RESULTS

***S. pombe* APC/C Stably Interacts with Both Mad2 and Mad3**—Our previous TAP of the APC/C from asynchronously growing *S. pombe* identified 13 core subunits (31). Using the TAP-tagged Lid1(Apc4) subunit, we purified APC/C from cells arrested in prometaphase using the *nda3-KM311* cold-sensitive tubulin allele. The *nda3-KM311* mutant has no microtubules at 18 °C and arrests with hypercondensed chromosomes due to spindle checkpoint activation (32). All other APC/C subunits identified previously (31) co-purified with Lid1, along with the Cdc20 activator (Fig. 1A). Strikingly, this mitotic APC/C also contained the Mad2 and Mad3 spindle checkpoint proteins. In a reverse experiment, Mad2, Cdc20, and all 13 core APC/C subunits were detected in a Mad3-TAP eluate purified from *nda3* arrested cells. No Mad1 or Bub (budding uninhibited by benzimidazole) proteins were detected in these complexes. These results, which were confirmed by immunoprecipitation and blotting (Fig. 1B), indicate that both Mad2 and Mad3 can stably interact with the APC/C in *S. pombe*. The stable associations we detected by TAP and mass spectrometry allowed us to address the mechanism by which Mad2 and Mad3 interact with the core APC/C in *S. pombe*.

Mad3 and Mad2 Interact with the APC/C Every Mitosis—We also found that Mad3 and Mad2 are stably associated with the

Mad3 KEN Box-mediated Cdc20-APC Binding

APC/C in an *mts3-1* mutant arrest (33). *mts3-1* arrests in a metaphase-like state due to decreased proteasome activity and the stabilization of securin and cyclin B (34). These cells are not sensitive to microtubule destabilizing agents, and components of the SAC do not accumulate on kinetochores in *mts3-1* cells (data not shown). This shows that Mad3 and Mad2 associate with the APC/C in a mitotic arrest that is independent of spindle checkpoint signaling. This was confirmed by accumulating cells in mitosis through overexpression of the N-terminal 70 amino acids of *S. pombe* cyclin B that lacks lysines (N70-K0; see "Experimental Procedures"). N70-K0 competes with endogenous APC/C substrates (35), and cells accumulate in metaphase independently of spindle checkpoint action. We could reproducibly detect both Mad2 and Mad3 bound to APC/C in N70-K0-induced mitotic delays (see Figs. 3 and 4).

To determine whether the Mad protein-APC/C complex assembles and disassembles during every cell cycle, we used the *cdc25* mutant to presynchronize cultures in G₂. Cells were then released from the block point, and samples were taken at 15-min intervals. Mad2 was immunoprecipitated, and we looked for associated Cdc20 and APC/C proteins by immunoblotting. Mad2 was found to associate with the APC/C specifically during mitosis (Fig. 2A). Similarly, during an *nda3* release time course, Lid1-Myc was detectable in a Mad2 immunoprecipitate up until the point of septation (Fig. 2B).

Sucrose gradient fractionation was carried out of extracts made from *nda3* arrested cells. Pools of Mad2, Mad3-GFP, and Cdc20/Slp1-HA were seen to co-fractionate with Lid1-TAP (Fig. 2C).

To determine what fraction of the total APC/C pool associates with checkpoint proteins, we made extracts from *nda3-KM311* and *mts3-1* arrested cells, immunodepleted Mad2 tagged at its endogenous locus with HTB using magnetic streptavidin beads (Fig. 2D, left panels), and quantitatively analyzed the amount of Lid1 associated with the beads and in the supernatant (see "Experimental Procedures"). We found that up to 8% of the APC/C was co-depleted with Mad2 (Fig. 2D, right panel). Thus, the levels of checkpoint proteins associated with APC/C increase specifically in mitosis and are significant, with at least 5% of the core APC/C bound by Mad2.

Mad3-KEN20, Cdc20, and Mad2 Mediate the Mad3-APC/C Interaction—How is the Mad3-APC/C interaction mediated? First, Mad3 interaction with the APC/C was observed to be dependent on Cdc20. The conditional *cdc20* allele, *slp1-362*, arrests in a metaphase-like state because the mutant Slp1-362 protein is unable to bind the APC/C at restrictive temperature (36). In a Lid1-TAP from this mutant, Slp1-362, Mad3, and Mad2 were all undetectable by mass spectrometry (33). Immunoblotting confirmed these mass spectrometry results; Lid1-TAP pull downs from N70-K0-overproducing cells contained both Mad3 and Mad2, but the pull down from mitotic *slp1-362* cells did not (Fig. 3A). We conclude that stable checkpoint protein interactions with the mitotic APC/C are Cdc20-dependent.

Cdc20 recognizes destruction (D) boxes and KEN boxes of APC/C substrates. Sequence analysis of Mad3 from different

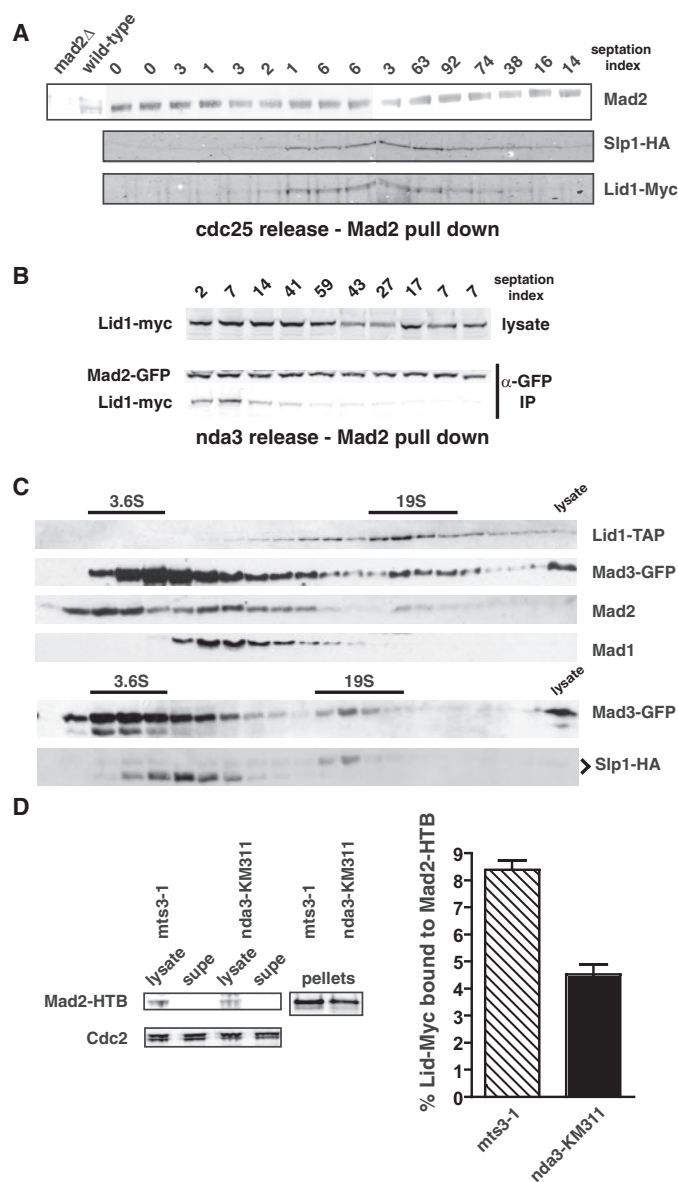


FIGURE 2. The Mad-APC/C complex is formed every mitosis. A, *cdc25* cultures were synchronized in G₂ and then released at 25 °C. Samples were taken at 15-min time points throughout mitosis, Mad2 was immunoprecipitated, immunoprecipitates were separated by SDS-PAGE, and then immunoblotted for associated Cdc20/Slp1-HA and Lid1-Myc. B, *nda3-KM311* cells were released from their early mitotic arrest, time points were taken, and Mad2-GFP was immunoprecipitated from extracts and then immunoblotted for Mad2 and associated Lid1. IP, immunoprecipitate. C, lysates from *nda3-KM311* arrested cells were fractionated on 10–40% sucrose gradients. Pools of Mad3-GFP, Mad2, and Cdc20/Slp1-HA were found to co-fractionate with Lid1-TAP in the 19 S size range. Thyroglobulin (19 S) and ovalbumin (3.6 S) were used as markers. D, lysates from arrested *mts3-1* or *nda3-KM311* cells containing Mad2-HTB and Lid1-Myc₁₃ were quantitatively depleted for Mad2 using magnetic streptavidin beads (left panel). The amount of Lid1-Myc₁₃ remaining in each lysate was determined by immunoblotting and quantification on an Odyssey machine (right panel). The average remaining was plotted as a percentage of the amount present in the initial lysates determined in an identical manner from six experiments performed on two separate occasions. *supe*, supernatant.

organisms revealed two conserved KEN boxes (Fig. 3B). To study their potential role in mediating an interaction with Cdc20-APC/C, we made three mutants in which the KEN boxes were replaced by a triple alanine (AAA) substitution: *mad3-KEN20AAA*, *mad3-KEN271AAA*, and *mad3-KEN20/271AAA*. The mutant proteins are present at wild-type levels

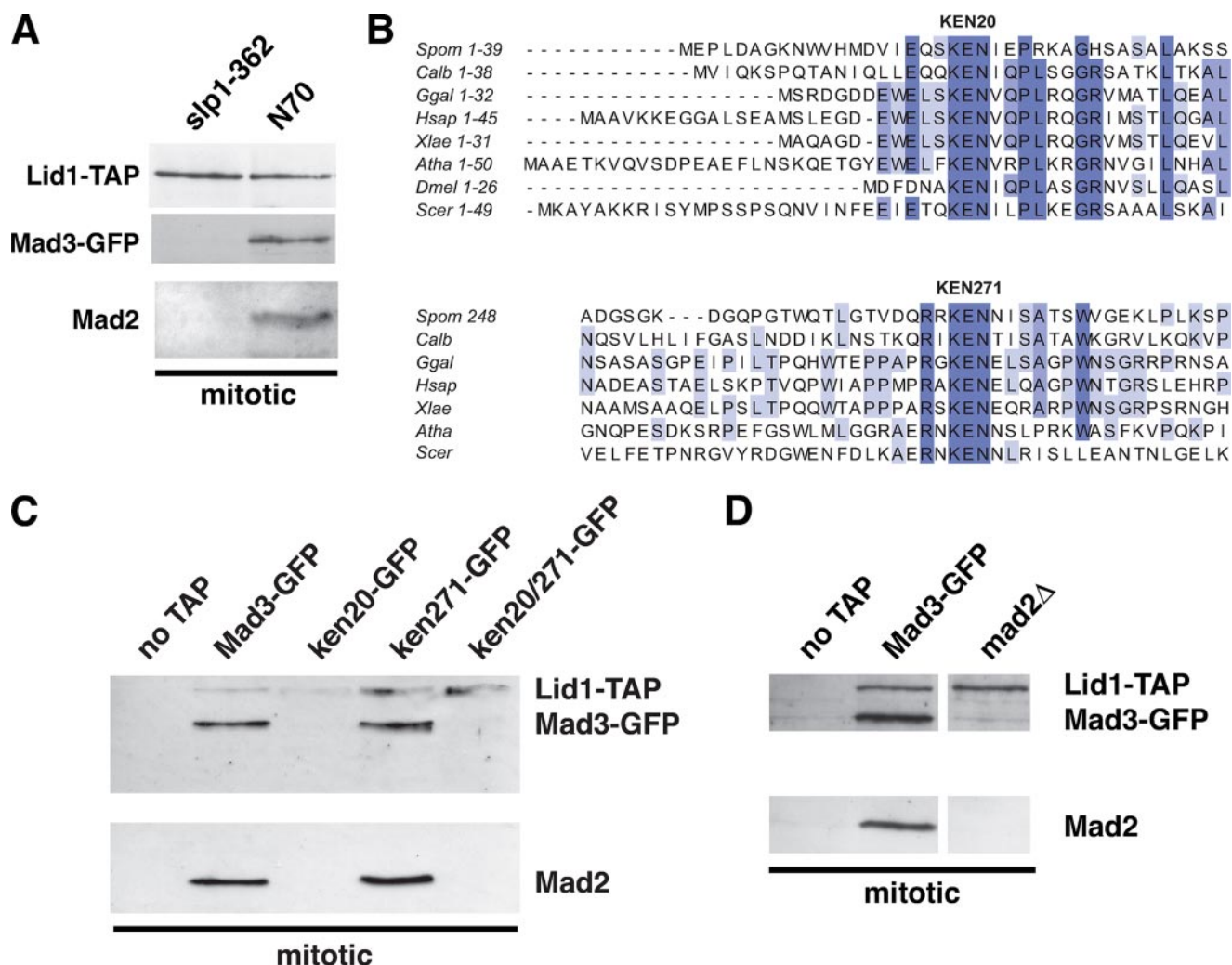


FIGURE 3. The *mad3-KEN20AAA* mutation abolishes stable APC/C association of both Mad3 and Mad2. **A**, wild-type and *slp1-362* strains were arrested at metaphase. APC/C was pulled down via Lid1-TAP using IgG Dynabeads and immunoblotted for Mad3-GFP and Mad2. **B**, the Mad3 and BubR1 proteins contain two conserved KEN boxes. Clustal alignments are shown for *S. pombe* (*Spom*), *Candida albicans* (*Calb*), *Gallus gallus* (*Ggal*), *Homo sapiens* (*Hsap*), *Xenopus laevis* (*Xlae*), *Arabidopsis thaliana* (*Atha*), *Drosophila melanogaster* (*Dmel*), and *S. cerevisiae* (*Scer*) Mad3/BubR1. **C**, the indicated *mad3* strains were arrested at metaphase using N70-K0. APC/C was pulled down via Lid1-TAP using IgG Dynabeads and immunoblotted for Mad3 and Mad2. **D**, similar Lid1 pull downs were performed from N70-K0-arrested wild-type and *mad2Δ* strains.

and can be recruited to kinetochores (Figs. 4 and 5), so mutation of these residues does not lead to gross changes in stability of the Mad3 protein or its localization. The *mad3-KEN* mutants were enriched in mitosis with N70-K0, Lid1-TAP was pulled down, and the associated Mad proteins were analyzed by immunoblotting. The *mad3-KEN20AAA* mutant abolished Mad3, and importantly also Mad2, association with the APC/C, whereas the *mad3-KEN271AAA* mutant had little effect (Fig. 3C and supplemental Fig. S1). As expected, the double KEN box mutant abolished APC/C binding. Very similar results were obtained using *mad3-KEN mts3-1* mutants (supplemental Fig. S2). Thus, Mad3- and Mad2-APC/C association is dependent on the highly conserved N-terminal KEN box that is found in Mad3 and BubR1.

Mad2 interaction with the APC/C is most likely bridged by direct interaction with Cdc20 (9, 10). To determine whether Mad3 requires Mad2 to stably bind the APC/C, we overproduced N70-K0 in *mad2Δ* cells so that they accumulate in mitosis,

pulled down Lid1-TAP, and immunoblotted for Mad3-GFP. Mad3-APC/C binding was Mad2-dependent (Fig. 3D). Thus, Mad3 is dependent on its own N-terminal KEN box, Mad2, and Cdc20 for APC/C association. Unexpectedly, Mad2 is also dependent on the N-terminal Mad3 KEN box for stable APC/C association (Fig. 3C). Thus, Mad2 and Mad3 are interdependent for stable APC/C binding.

KEN20 Mediates Cdc20 Binding and MCC Formation—Mad3 is part of the MCC, which in fission yeast is comprised exclusively of Mad3, Mad2, and Cdc20. In other organisms, Bub3 is also a component of the MCC. However, *S. pombe* Mad3 lacks the GLEBS motif that is necessary and sufficient for *Saccharomyces cerevisiae* Mad3 to bind Bub3 (37). Thus, although Bub3 is important for the kinetochore targeting of Mad3 (28, 38), Bub3 is not stably associated with either MCC or APC/C in fission yeast (Fig. 1A and data not shown).

Due to the co-dependence of Mad2 and Mad3 for stable APC/C association, we considered the possibility that this stable association requires formation of the MCC. To test

Mad3 KEN Box-mediated Cdc20-APC Binding

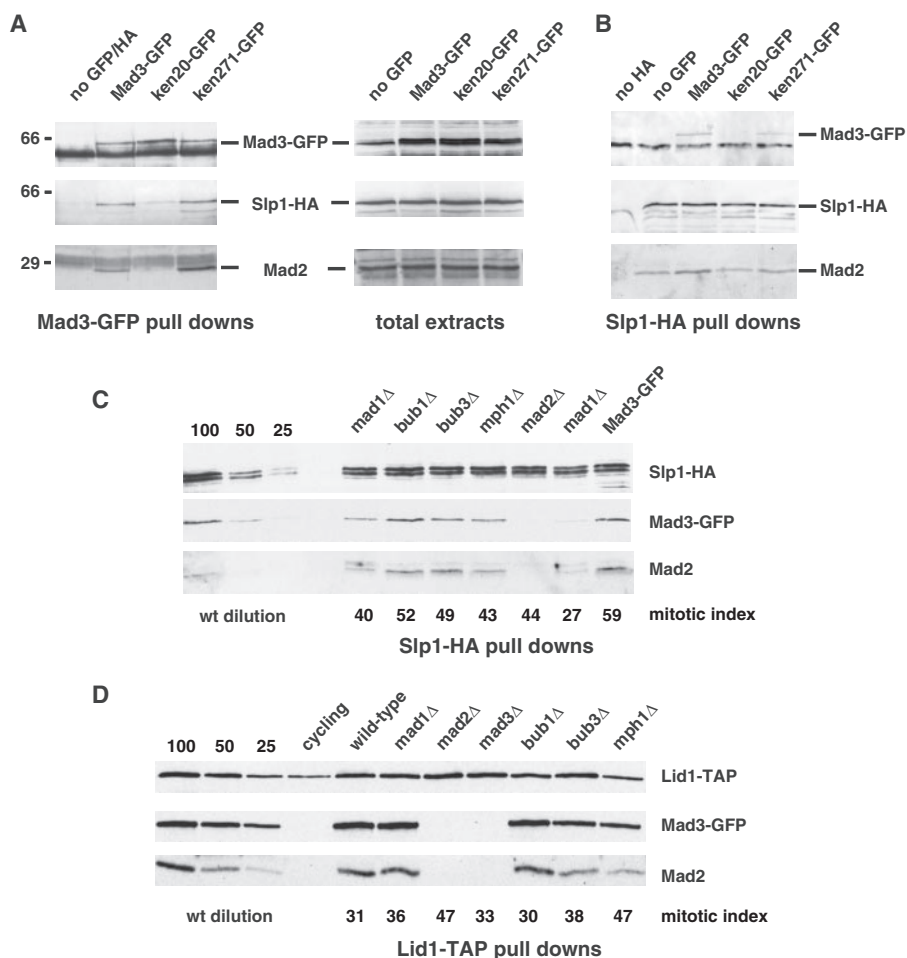


FIGURE 4. The *mad3*-KEN20AAA mutation abolishes MCC formation, whereas upstream checkpoint signaling components are not necessary. *A*, strains were arrested at metaphase through overexpression of the N terminus of cyclin (N70-K0), and arrests were scored by mitotic spindle staining. Mad3-GFP was immunoprecipitated from mitotic extracts, separated by SDS-PAGE, and then immunoblotted for Mad3, Cdc20/Slp1, and Mad2. *B*, the same strains were arrested, extracts were made, and Cdc20/Slp1-HA was immunoprecipitated and then immunoblotted for Cdc20/Slp1, Mad3-GFP, and Mad2. Note that the *mad3*-KEN20AAA mutation did not perturb Mad2-Cdc20 association. *C*, mutant strains (*mad1*, *mad2*, *bub1*, *bub3*, and *mph1*) were arrested at metaphase through overexpression of the N terminus of cyclin (N70-K0). The mitotic index was scored by mitotic spindle staining with anti-tubulin antibodies. Cdc20/Slp1-HA was immunoprecipitated from mitotic extracts, separated by SDS-PAGE, and then immunoblotted for Cdc20/Slp1-HA, Mad3-GFP, and Mad2. The first three lanes are loading controls, where 100, 50, and 25% of the wild-type (*wt*) (Mad3-GFP) sample were loaded for comparison. *D*, Lid1 pull downs (using IgG Dynabeads) were performed from N70-K0-arrested checkpoint mutants and immunoblotted for Lid1-TAP, Mad3-GFP, and Mad2. The mitotic index was scored by mitotic spindle staining.

the importance of the Mad3 KEN boxes for MCC formation, we enriched for mitotic wild-type and *KEN* mutant cells in mitosis using N70. We then carried out immunoprecipitations of Mad3-GFP and Cdc20/Slp1-HA from these mitotic extracts and found that mutation of the N-terminal KEN box (*mad3*-KEN20AAA) abolished the interaction between Mad3 and both Cdc20 and Mad2, demonstrating that it is necessary for MCC formation (Fig. 4, *A* and *B*). Mutation of the C-terminal KEN box (*mad3*-KEN271AAA) did not have this effect on Cdc20 or Mad2 binding. It is important to note here that neither the *mad3*-KEN20AAA mutation (Fig. 4*B*) nor deletion of *mad3* (data not shown) interfered with Mad2-Cdc20 binding. This contrasts with its effect on Mad2-APC/C binding, which was abolished in *mad3*-KEN20AAA (Fig. 3*C*), and supports our proposal that check-

point protein-APC/C association requires the integrity of the MCC *in vivo* (Fig. 6*A*).

MCC Formation Is Independent of Upstream Checkpoint Signaling and Kinetochores Targeting—It has been demonstrated that budding yeast MCC forms independently of kinetochores. For example, in *ndc10-1* mutants, where kinetochores are completely absent at restrictive temperatures, the MCC assembles with normal kinetics and to normal levels (39, 40). We attempted similar experiments with the fission yeast *nuf2-1* allele (41), but these cells were too sick for detailed biochemistry. Instead, we analyzed the MCC in fission yeast strains lacking Bub3, Bub1, Mph1, and Mad1. These proteins are critical for kinetochores targeting of other checkpoint components; Bub3 and Bub1 are both required for Mad3 localization (38, 42), and Mad1 is necessary for Mad2 recruitment to fission yeast kinetochores (43). In all of these mutants, which were enriched in mitotic cells due to N70 overexpression, we could readily detect an interaction between Mad2, Mad3, and Cdc20 (Fig. 4*B*). The only mutant demonstrating significant quantitative reduction in MCC levels was *mad1*, and in this case, the effect was typically only 2–3-fold (Fig. 4*B*). This experiment demonstrates that fission yeast MCC can be formed independently of upstream checkpoint signaling components and that kinetochores targeting of the MCC components is not necessary for its

assembly. Similar experiments, pulling down Lid1-TAP, showed that the Mad2 and Mad3 interaction with the APC/C was also independent of these upstream factors (Fig. 4*C*, and data not shown). It is important to note that although MCC and MCC-APC/C are still being assembled in these fission yeast mutants, the checkpoint is not functional and Cdc20-APC/C is not efficiently inhibited.

Mad3 KEN Boxes Are Required for Spindle Checkpoint Function—Three assays were employed to test the functional requirement for Mad3-KEN boxes in spindle checkpoint signaling. First, we made *nda3*-KM311 *mad3*-KEN-AAA double mutants and assayed their ability to arrest and maintain viability at 18 °C. Both *KEN* mutants behaved like the *mad3* Δ strain in this assay; cells failed to arrest with condensed chromosomes, mis-segregated their DNA, displayed the cut (*cells*

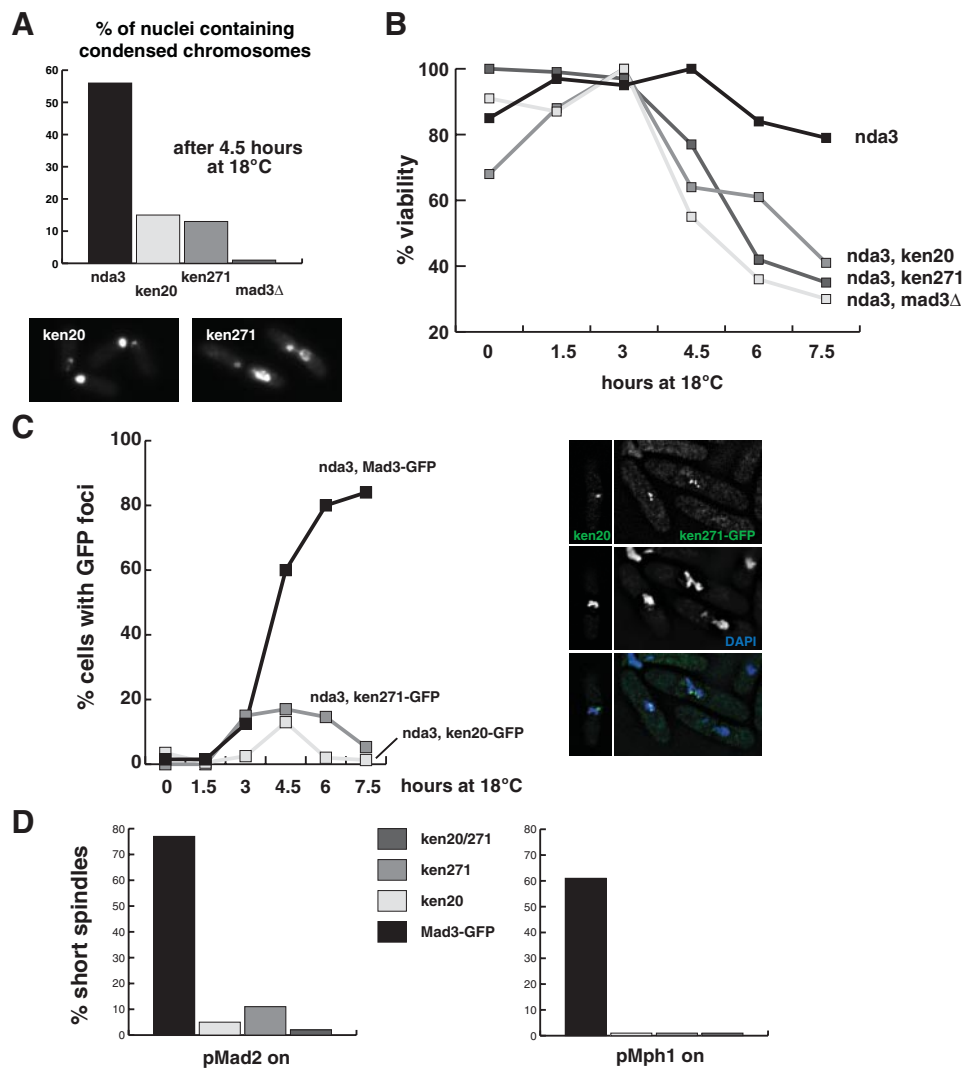


FIGURE 5. Mutation of Mad3 KEN boxes abolishes spindle checkpoint arrests. *A*, *nda3-KM311* cultures were shifted to their restrictive temperature (18 °C), and cells were analyzed microscopically for chromosome condensation and mis-segregation. Images of the *KEN* mutants, taken at the 6-h time point, are of DAPI-stained cells and demonstrate severe segregation defects and *cut* cells. The scale bar is 5 μm. *B*, cells were taken from these cultures and plated at the indicated time points. Viability was scored as colony formation. *C*, the *nda3-KM311* strains were scored for the formation of Mad3-GFP foci (kinetochores) at the indicated time points. The inset images show Mad3-GFP (green) and chromosomes (DAPI, blue). *D*, Mad2 and Mph1 overexpression arrests were scored by counting short metaphase spindles after 16 h of Mad2 or Mph1 induction from the *nmt* promoter. The *KEN* mutants fail to accumulate metaphase cells, confirming that they are checkpoint-defective.

untimely torn) phenotype (Fig. 5A), and lost viability rapidly after 3 h at 18 °C (Fig. 5B). During this experiment, we also analyzed the recruitment of GFP-tagged *mad3 KEN* mutant proteins to kinetochores. The Mad3 KEN mutant proteins were recruited to kinetochores. However, quantitation of the numbers of cells with bright Mad3-GFP foci during the *nda3-KM311* time course confirmed that the *KEN* mutants were unable to arrest in mitosis as the mutant cultures failed to accumulate cells with bright Mad3-GFP foci (Fig. 5C).

Mad2 or Mph1 overexpression arrests wild-type *S. pombe* cells at metaphase (44, 45), and this was scored by staining cells with anti-tubulin antibodies and counting mitotic spindles in cultures overproducing these proteins. When Mad2 or Mph1 was overexpressed in the *mad3 KEN* mutants, they showed a greatly decreased ability to arrest at metaphase. This arrest was scored by staining cells with anti-tubulin

antibodies and counting the frequency of mitotic spindles (Fig. 5D). Thus, using three independent assays, we find that mutation of Mad3 KEN boxes abrogates spindle checkpoint arrests.

DISCUSSION

Our findings demonstrate the importance of Mad3, and in particular, its conserved N-terminal KEN box, for MCC formation, for APC/C binding, and for inhibition of anaphase by the SAC. Mad2 and Mad3/BubR1 are direct inhibitors of Cdc20 function; *in vitro*, either is sufficient to inhibit Cdc20-APC/C (27, 46), and they are more potent when combined (30). *In vivo*, it is far from clear whether distinct anaphase inhibitors exist, although distinct complexes certainly do (40). To date, the mechanism of Mad2 function has received far more attention than that of Mad3/BubR1, and structural studies of Mad2-Cdc20 (and Mad2-Mad1) are beginning to explain how this complex is formed and how it might contribute to checkpoint signal propagation (21, 23, 24). Less is known about Mad3/BubR1 interactions with Cdc20-APC/C, although *in vitro* studies have suggested the existence of multiple Cdc20 binding sites for Mad3 (25, 27, 47).

Here we have identified the N-terminal Mad3 KEN box as a mediator of interactions that are crucial for checkpoint function and have highlighted the importance of Mad3/BubR1 as an anaphase inhib-

itor. We have demonstrated that the KEN20 motif is absolutely necessary for a detectable interaction between Mad3 and Cdc20. We and others recently reported similar findings in budding yeast (48, 49). Importantly, our fission yeast studies demonstrate that KEN20 is also necessary for detectable interaction between Mad3 and the APC/C and between Mad2 and the APC/C. Our fission yeast data also highlight an interdependence between Mad3 and Mad2 for detectable APC/C interaction; neither checkpoint protein stably binds the APC/C in the absence of the other, and neither binds when Mad3 *KEN20* is mutated. We have previously demonstrated that the ability of Mad2 overexpression to arrest *S. pombe* cells in mitosis (45) is dependent on Mad3 (28). This can now be explained as overexpressed Mad2 will not associate with the core APC/C in the absence of Mad3, although it can bind Cdc20. These data

Mad3 KEN Box-mediated Cdc20-APC Binding

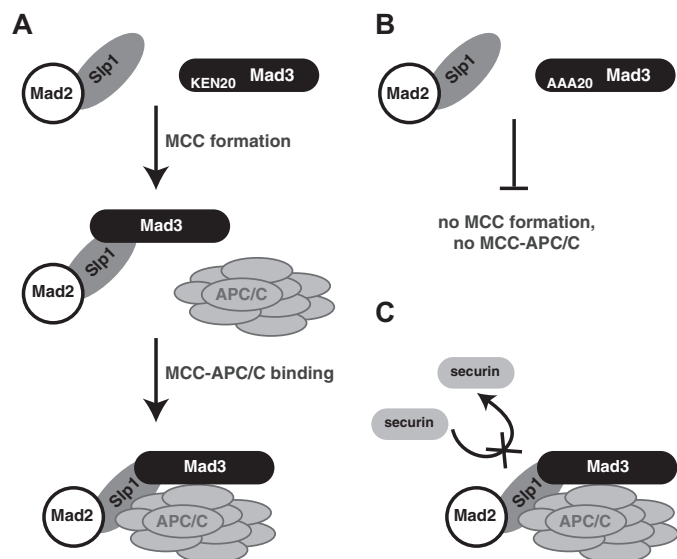


FIGURE 6. Models of Mad3 interactions. *A*, model of stepwise assembly of the checkpoint protein APC/C complex. Note that this model is based on genetic dependencies and does not necessarily imply that this order of assembly would be observed during biochemical reconstitution. *B*, mutation of KEN20 abolishes MCC formation and thereby prevents APC/C interactions for both Mad3 and Mad2. *C*, Cdc20/Slp1-APC/C inhibition by Mad3 and Mad2 could result from several distinct mechanisms. These include pseudo-substrate action of Mad3/Mad2, non-productive substrate binding, or a block in substrate release.

strongly argue against Mad2-Cdc20 being an efficient anaphase inhibitor *in vivo* and highlight the importance of the MCC for full APC/C inhibition. This is concordant with findings from *Xenopus* and *in vitro* studies that describe cooperative interactions between BubR1 and Mad2 in Cdc20-APC/C binding and inhibition (30, 47, 50).

We describe the Mad2-Mad3-Cdc20-APC/C interactions we have identified as stable, based on their maintenance through various biochemical purification strategies. However, it is possible that our estimates of the abundance of these complexes (5–10% of the APC/C was immunodepleted with Mad2, Fig. 2*D*) is minimal, particularly if they are highly dynamic in cells. Even so, it is likely that additional modes of checkpoint protein action are employed for full APC/C inhibition.

Mad2 and Mad3 association with the core APC/C is dependent on the Cdc20 activator. Indeed, all of our APC/C interaction data are consistent with a relatively straightforward model in which Mad3 and Mad2 interact with the APC/C indirectly via Cdc20, most simply in the form of the MCC (Fig. 6*A*). Mutation of KEN20 blocks MCC formation and thereby prevents APC/C interactions (Fig. 6*B*). As mentioned, stable interactions between Mad3, Mad2, and the APC/C are not restricted to fission yeast. An association between Mad2 and specific vertebrate APC/C subunits (46, 51, 52) and a regulated BubR1-APC/C interaction (53) have been previously reported. Surprisingly, there appears to be little detectable checkpoint protein interaction with the APC/C in *S. cerevisiae* (54).⁶ Whether this reflects different modes of APC/C inhibition in the two yeast, or just different dynamics of the APC/C interaction, remains to be seen.

The association of BubR1 with the vertebrate APC/C was

⁶ K. G. Hardwick, unpublished data.

shown to be dependent on checkpoint signaling (53). When the checkpoint was turned off, but cells were still trapped in mitosis through treatment with the proteasome inhibitor (MG132), the complex was no longer apparent. Formation of the BubR1-APC/C complex in response to taxol treatment required Aurora B activity, and in response to nocodazole treatment, it required Bub1 activity (53). In our experiments, we saw significant Mad3-APC/C binding in cells overproducing N70-K0 and the *mts3* proteasome mutant arrest, so a requirement for spindle checkpoint signaling is far less apparent. However, we cannot rule out that there is a quantitative effect on the Mad-APC/C complexes upon checkpoint activation or that they are modified in an as yet unidentified way.

In addition, we have analyzed the dependence of Mad3-Mad2-Cdc20 interactions and Mad3-APC/C binding on other checkpoint proteins. Formation of both complexes was independent of Bub3, Bub1, Mph1, and Mad1 functions (Fig. 4, *B* and *C*). Thus, these interactions can occur in fission yeast mitosis independently of spindle checkpoint signaling and independently of kinetochore recruitment of Mad3 as that is entirely abolished in *bub3Δ* and *bub1Δ* strains (38, 42). We propose that MCC formation and APC/C binding take place in the nucleoplasm every mitosis, independently of kinetochore-based SAC signaling. If this proves to be the case, it is reminiscent of the “mitotic timer function,” proposed for human Mad2 and BubR1, that is essential to restrain anaphase onset in early mitosis when kinetochores are still assembling (55). There is evidence in fission yeast that mitosis is a little shorter in the absence of Mad2 function (56), consistent with a timing function for MCC proteins in this system.

It is important to note that although fission yeast MCC and MCC-APC/C complexes can be assembled independently of upstream signaling components (for example in *mad1* or *bub1* mutants) and kinetochore targeting, these complexes are not capable of checkpoint arrest. We propose that one or more MCC components lack critical post-translational modifications, without which they fail to function as efficient anaphase inhibitors. These modifications may be added at kinetochores during the dynamic exchange of Mad2, Mad3, and/or Cdc20. Ongoing work aims to test this hypothesis.

There are several ways that Mad3 might inhibit Cdc20-APC/C (Fig. 6*C*). The simplest scenario would be for Mad3 binding to prevent securin from interacting with Cdc20-APC/C prior to anaphase onset. In this model, Mad3 would act as a competitive “pseudo-substrate.” Such a mode of action was recently proposed for the Emi1 APC/C inhibitor (57) and for budding yeast Mad3 (48). However, two observations argue against such a model for Mad3 in fission yeast. First, a prediction of this model is that overexpression of the pseudo-substrate should induce a metaphase arrest, yet overexpression of Mad3 does not induce a metaphase arrest in either *S. pombe* or *S. cerevisiae* (data not shown) (49, 58). Second, Mad3 and N70-K0 (the Cdc13 destruction box) do not appear to compete for Cdc20-APC/C interaction in our *in vivo* experiments, as we were able to co-immunoprecipitate Mad3 and the APC/C from N70 arrested cells (Figs. 1–3). Alternative models for Mad3 function include non-productive substrate binding, where

Mad3 does not prevent securin-APC/C interaction but does block ubiquitin transfer or perhaps an ability to block substrate release.

Importantly, the *mad3-KEN271AAA* allele indicates that building MCC and MCC-APC/C complexes is not sufficient for checkpoint arrest. This *mad3* mutant assembles into both of these complexes, but they appear to lack potency, and the checkpoint arrest is severely defective. Further experiments are necessary to understand and dissect the complexity of Mad3 action.

Perhaps our most striking finding is that the N-terminal Mad3 KEN box is being used to mediate stable Cdc20-APC/C binding and inhibition rather than as a mitotic degron. D boxes and KEN boxes can determine the order in which mitotic APC/C substrates are degraded and do this by determining processivity of ubiquitination (59). Fission yeast Mad3 is stable in mitosis (see supplemental Fig. S3, as it is in budding yeast (49)), so we propose that it is a relatively poor “ubiquitin acceptor” and that it is not ubiquitinated in a processive manner.

It has been shown that BubR1 kinase activity has important roles in mediating both checkpoint activation and silencing in vertebrates, and this is regulated by interactions with the kinesin-like protein CENP-E (29). Several organisms, including yeasts and *Caenorhabditis elegans*, lack this C-terminal kinase domain, yet Mad3 is still very important for the spindle checkpoint. Here we have demonstrated that the N-terminal Mad3 KEN box, conserved from yeast to BubR1 in human, is a critical mediator of Cdc20-APC/C inhibition.

Acknowledgments—We thank Hiro Yamano and Shelley Sazer for overexpression constructs (*N70-K0*, *Mad2* and *Mph1*), Tomohiro Matsumoto for *slp1-362*, Peter Kaiser for the *HTB* tagging cassette, and Colin Gordon for *mts3-1*.

REFERENCES

1. Hassold, T., and Hunt, P. (2001) *Nat. Rev. Genet.* **2**, 280–291
2. Musacchio, A., and Salmon, E. D. (2007) *Nat. Rev. Mol. Cell Biol.* **8**, 379–393
3. Cleveland, D. W., Mao, Y., and Sullivan, K. F. (2003) *Cell* **112**, 407–421
4. Taylor, S. S., Scott, M. I., and Holland, A. J. (2004) *Chromosome Res.* **12**, 599–616
5. Peters, J. M. (2006) *Nat. Rev. Mol. Cell Biol.* **7**, 644–656
6. Visintin, R., Prinz, S., and Amon, A. (1997) *Science* **278**, 460–463
7. Kitamura, K., Maekawa, H., and Shimoda, C. (1998) *Mol. Biol. Cell* **9**, 1065–1080
8. Kominami, K., Seth-Smith, H., and Toda, T. (1998) *EMBO J.* **17**, 5388–5399
9. Kim, S. H., Lin, D. P., Matsumoto, S., Kitazono, A., and Matsumoto, T. (1998) *Science* **279**, 1045–1047
10. Hwang, L. H., Lau, L. F., Smith, D. L., Mistrot, C. A., Hardwick, K. G., Hwang, E. S., Amon, A., and Murray, A. W. (1998) *Science* **279**, 1041–1044
11. Cohen-Fix, O. (1996) *Genes Dev.* **10**, 3081–3093
12. Shirayama, M., Toth, A., Galova, M., and Nasmyth, K. (1999) *Nature* **402**, 203–207
13. Thornton, B. R., and Toczyski, D. P. (2003) *Nat. Cell Biol.* **5**, 1090–1094
14. Glotzer, M., Murray, A. W., and Kirschner, M. W. (1991) *Nature* **349**, 132–138
15. Pflieger, C. M., and Kirschner, M. W. (2000) *Genes Dev.* **14**, 655–665
16. Burton, J. L., and Solomon, M. J. (2001) *Genes Dev.* **15**, 2381–2395
17. Hilioti, Z., Chung, Y. S., Mochizuki, Y., Hardy, C. F., and Cohen-Fix, O. (2001) *Curr. Biol.* **11**, 1347–1352
18. Burton, J. L., Tsakraklides, V., and Solomon, M. J. (2005) *Mol. Cell* **18**, 533–542
19. Kraft, C., Vodermaier, H. C., Maurer-Stroh, S., Eisenhaber, F., and Peters, J. M. (2005) *Mol. Cell* **18**, 543–553
20. Yamano, H., Gannon, J., Mahbubani, H., and Hunt, T. (2004) *Mol. Cell* **13**,

- 137–147
21. De Antoni, A., Pearson, C. G., Cimini, D., Canman, J. C., Sala, V., Nezi, L., Mapelli, M., Sironi, L., Faretta, M., Salmon, E. D., and Musacchio, A. (2005) *Curr. Biol.* **15**, 214–225
22. Nasmyth, K. (2005) *Cell* **120**, 739–746
23. Yu, H. (2006) *J. Cell Biol.* **173**, 153–157
24. Mapelli, M., Massimiliano, L., Santaguida, S., and Musacchio, A. (2007) *Cell* **131**, 730–743
25. Hardwick, K. G., Johnston, R. C., Smith, D. L., and Murray, A. W. (2000) *J. Cell Biol.* **148**, 871–882
26. Sudakin, V., Chan, G. K., and Yen, T. J. (2001) *J. Cell Biol.* **154**, 925–936
27. Tang, Z., Bharadwaj, R., Li, B., and Yu, H. (2001) *Dev. Cell* **1**, 227–237
28. Millband, D. N., and Hardwick, K. G. (2002) *Mol. Cell Biol.* **22**, 2728–2742
29. Mao, Y., Abrieu, A., and Cleveland, D. W. (2003) *Cell* **114**, 87–98
30. Fang, G. (2002) *Mol. Biol. Cell* **13**, 755–766
31. Yoon, H. J., Feoktistova, A., Wolfe, B. A., Jennings, J. L., Link, A. J., and Gould, K. L. (2002) *Curr. Biol.* **12**, 2048–2054
32. Hiraoka, Y., Toda, T., and Yanagida, M. (1984) *Cell* **39**, 349–358
33. Ohi, M. D., Feoktistova, A., Ren, L., Yip, C., Cheng, Y., Chen, J. S., Yoon, H. J., Wall, J. S., Huang, Z., Penczek, P. A., Gould, K. L., and Walz, T. (2007) *Mol. Cell* **28**, 871–885
34. Gordon, C., McGurk, G., Wallace, M., and Hastie, N. D. (1996) *J. Biol. Chem.* **271**, 5704–5711
35. Yamano, H., Tsurumi, C., Gannon, J., and Hunt, T. (1998) *EMBO J.* **17**, 5670–5678
36. Matsumoto, T. (1997) *Mol. Cell Biol.* **17**, 742–750
37. Larsen, N. A., Al-Bassam, J., Wei, R. R., and Harrison, S. C. (2007) *Proc. Natl. Acad. Sci. U. S. A.* **104**, 1201–1206
38. Vanoosthuyse, V., Valsdottir, R., Javerzat, J. P., and Hardwick, K. G. (2004) *Mol. Cell Biol.* **24**, 9786–9801
39. Fraschini, R., Beretta, A., Sironi, L., Musacchio, A., Lucchini, G., and Piatti, S. (2001) *EMBO J.* **20**, 6648–6659
40. Poddar, A., Stukenberg, P. T., and Burke, D. J. (2005) *Eukaryot. Cell* **4**, 867–878
41. Nabetani, A., Koujin, T., Tsutsumi, C., Haraguchi, T., and Hiraoka, Y. (2001) *Chromosoma (Berl.)* **110**, 322–334
42. Kadura, S., He, X., Vanoosthuyse, V., Hardwick, K. G., and Sazer, S. (2005) *Mol. Biol. Cell* **16**, 385–395
43. Ikui, A. E., Furuya, K., Yanagida, M., and Matsumoto, T. (2002) *J. Cell Sci.* **115**, 1603–1610
44. He, X., Jones, M. H., Winey, M., and Sazer, S. (1998) *J. Cell Sci.* **111**, 1635–1647
45. He, X., Patterson, T. E., and Sazer, S. (1997) *Proc. Natl. Acad. Sci. U. S. A.* **94**, 7965–7970
46. Fang, G., Yu, H., and Kirschner, M. W. (1998) *Genes Dev.* **12**, 1871–1883
47. Davenport, J., Harris, L. D., and Goorha, R. (2006) *Exp. Cell Res.* **312**, 1831–1842
48. Burton, J. L., and Solomon, M. J. (2007) *Genes Dev.* **21**, 655–667
49. King, E. M., van der Sar, S. J., and Hardwick, K. G. (2007) *PLoS ONE* **2**, e342
50. Chen, R. H. (2002) *J. Cell Biol.* **158**, 487–496
51. Kallio, M., Weinstein, J., Daum, J. R., Burke, D. J., and Gorbsky, G. J. (1998) *J. Cell Biol.* **141**, 1393–1406
52. Braunstein, I., Miniowitz, S., Moshe, Y., and Hershko, A. (2007) *Proc. Natl. Acad. Sci. U. S. A.* **104**, 4870–4875
53. Morrow, C. J., Tighe, A., Johnson, V. L., Scott, M. I., Ditchfield, C., and Taylor, S. S. (2005) *J. Cell Sci.* **118**, 3639–3652
54. Camasses, A., Bogdanova, A., Shevchenko, A., and Zachariae, W. (2003) *Mol. Cell* **12**, 87–100
55. Meraldi, P., Draviam, V. M., and Sorger, P. K. (2004) *Dev. Cell* **7**, 45–60
56. Tange, Y., and Niwa, O. (2007) *Genetics* **175**, 1571–1584
57. Miller, J. J., Summers, M. K., Hansen, D. V., Nachury, M. V., Lehman, N. L., Loktev, A., and Jackson, P. K. (2006) *Genes Dev.* **20**, 2410–2420
58. Warren, C. D., Brady, D. M., Johnston, R. C., Hanna, J. S., Hardwick, K. G., and Spencer, F. A. (2002) *Mol. Biol. Cell* **13**, 3029–3041
59. Rape, M., Reddy, S. K., and Kirschner, M. W. (2006) *Cell* **124**, 89–103
60. Tagwerker, C., Zhang, H., Wang, X., Larsen, L. S., Lathrop, R. H., Hatfield, G. W., Auer, B., Huang, L., and Kaiser, P. (2006) *Yeast* **23**, 623–632